

Constraints on a soft X-ray excess in the quasar 3C 279

A. J. Lawson and I. M. McHardy

Department of Physics & Astronomy, University of Southampton, University Road, Southampton SO17 1BJ

Accepted for publication by MNRAS, 1998 July 3.

ABSTRACT

We present the results of a three-week daily monitoring campaign on the quasar 3C 279 by the X-ray satellites *RXTE* and *ROSAT*. A cross correlation provides no evidence for any time lag between the very similar soft and hard X-ray light curves, and the source shows no significant spectral variability over the observing period. There is no evidence to support the presence of a soft excess, with a 99 per cent upper limit on any such component of 25 per cent of the total observed luminosity in the 0.1–2 keV band ($< 3 \times 10^{38}$ W). This fraction (but not the luminosity) is significantly less than that of the soft excess observed in 3C 273.

Key words: quasars: individual: 3C 279 - galaxies: active - X-rays: galaxies

1 INTRODUCTION

Soft excesses are the steep upturn in the X-ray spectra of active galactic nuclei (AGN) below ~ 2 keV (e.g. Mushotzky, Done & Pounds 1993). They were first detected in Seyfert galaxies (Arnaud et al. 1985), where they are quite common (Turner & Pounds 1989; Mushotzky et al. 1993). They can be modelled by a steep power law ($\alpha > 2$), or by a cool thermal component ($T < 150$ eV), and are thought to be the high energy tail of the accretion disc radiation (e.g. Mushotzky et al. 1993).

Soft excesses are reasonably common in quasars (Urry et al. 1989; Masnou et al. 1992; Saxton et al. 1993), and there appears to be a trend for the more distant objects to have flatter spectra (Schartel et al. 1992), as expected if a soft component were being redshifted below the soft X-ray energy range. Initial detections were in radio-quiet objects (Comastri et al. 1992), but more recent work (Bühler et al. 1995; Prieto 1996; Schartel et al. 1996) suggests that a soft excess may also be a common feature in radio-loud objects. One of these with a consistently detected soft excess is 3C 273 (Turner et al. 1990; Staubert 1992; Leach, McHardy & Papadakis 1995). It is also one object for which the spectral parameters of the soft excess itself are reasonably well known (Leach et al. 1995).

2 THE *RXTE* AND *ROSAT* OBSERVATIONS

The main instrument on *RXTE* (Bradt, Rothschild & Swank 1993) is the proportional counter array (PCA). With five xenon filled counters (PCU's), it has an energy range of 2–60 keV, an energy resolution of 18 per cent at 6 keV, a large ($\sim 0.7\text{m}^2$) effective area, and a circular field of view (FWHM: 1°). Each PCU has three separate layers. Only data from

layer 1 has been used, as for observations of faint sources most of the counts in layers 2 and 3 are caused by the background. Problems with two of the PCUs meant they were switched off for some of the observations (noted in Table 1).

The *RXTE* observations (see Table 1) were made on a roughly daily basis between 1996 June 27 to July 14 and have an average exposure of about 650 seconds. Data reduction was done using *RXTE* specific *FTOOL* programs. The Standard2 data were filtered using internally applied good times (e.g. times of SAA passage), as well as the criteria that elevation above the horizon of greater than 10° and offsource angle of less than 0.1° , and then reduced to light curves and spectra using *SAEXTRACT*.

The PCA cannot measure the background during an observation and so it must be estimated. The accuracy of this estimation is very important for faint sources such as 3C 279. *PCABACKEST* (v1.4g with the q6 model) was used to produce models of the background due to particles and cosmic X-rays, and spectra and light curves were then extracted from these models in the same way as for the source observations. In order to check the accuracy of the PCA background model, and to provide a systematic error for the PCA datapoints, we have analysed 11 slew observations with individual exposures of greater than 400 seconds (average exposure is 671 seconds). The mean residual count rate after subtraction of the background in the ~ 2 –15 keV band is -0.25 cts/sec (i.e. the model is an over estimate of the data on average), with an intrinsic scatter of 0.44 cts/sec.

ROSAT observed 3C 279 17 times between 1996 June 28 and July 14 (see Table 1) using the *HRI*, an imager with an energy range of 0.1–2 keV, but no energy resolution. The data were analysed using *XSELECT*, part of the *FTOOL* software system. Counts were taken from a circular region 160 arcsec in radius centred on the source, while the background was derived from an annulus 160–320 arcsec from the source.

Table 1. Observational parameters

RXTE						ROSAT				
Obs ^a	Day and time ^b	Date ^c	Exp ^d	Det ^e	Count rate ^f	Obs ^a	Day and Time ^b	Date ^c	Exp ^d	Count rate
1	27/6 07:01:21	179.293	1152	5	6.25±0.17	1	28/6 08:59:35	180.375	1975	0.253±0.015
2	28/6 16:02:41	180.669	640	5	5.94±0.21	2	29/6 11:57:16	181.498	2387	0.264±0.014
3	29/6 11:16:09	181.470	704	3	5.94±0.25	3	30/6 07:09:45	182.298	2177	0.269±0.014
4	30/6 05:23:29	182.225	544	3	5.83±0.30	4	01/7 07:02:43	183.294	2070	0.307±0.015
5	01/7 06:29:13	183.270	720	3	5.82±0.25	5	02/7 06:55:30	184.289	2057	0.265±0.015
6	02/7 08:06:09	184.338	704	5	6.31±0.20	6	03/7 06:46:37	185.282	2113	0.267±0.014
7	03/7 12:55:21	185.538	688	5	5.13±0.20	7	04/7 06:38:45	186.277	2093	0.267±0.014
8	04/7 11:20:09	186.472	720	5	5.02±0.20	8	05/7 06:29:45	187.271	1977	0.253±0.014
9	05/7 06:33:37	187.273	544	3	5.48±0.29	9	06/7 07:54:21	188.329	2311	0.243±0.014
10	07/7 13:20:25	189.556	560	3	4.55±0.29	10	07/7 07:46:29	189.324	2231	0.220±0.014
11	09/7 16:45:53	191.699	736	3	4.36±0.27	11	08/7 04:28:53	190.187	2033	0.209±0.014
12	10/7 18:28:25	192.770	688	3	4.70±0.29	12	09/7 01:06:24	191.046	1768	0.238±0.015
13	11/7 19:25:21	193.810	544	5	5.21±0.24	13	10/7 00:57:44	192.040	1834	0.217±0.015
14	12/7 15:06:01	194.629	608	5	3.93±0.23	14	11/7 07:16:13	193.303	2238	0.215±0.013
15	13/7 09:57:13	195.415	576	3	3.93±0.29	15	12/7 00:42:46	194.030	1915	0.221±0.014
16	14/7 16:48:41	196.701	512	3	5.25±0.34	16	13/7 03:51:19	195.161	1963	0.178±0.013
						17	14/7 03:42:38	196.155	1901	0.231±0.014

Notes: ^aObservation No., ^bMiddle of the observation (UT), ^cWhere Jan 1st 1996 at 00:00:00 is day 1.0 (UT), ^dExposure (seconds) after data selection, ^eNo. of PCUs on during the observation, ^f2.19–15.5 keV band (spectral channels 2–36, systematic effects of the background modeling *not* included), when only three detectors were on the count rate has been corrected using PCU area ratios

3 LIGHT CURVES

Visual examination shows similar behaviour in both the *RXTE* and *HRI* light curves (Fig. 1). Both light curves display a slow, quasi-linear, decrease in intensity of approximately 30 per cent. A discrete cross-correlation does not provide any strong constraints, owing to the largely featureless nature of the light curves, and the two light curves are perfectly consistent with zero lag.

4 SPECTRAL ANALYSIS

4.1 Broad-band comparisons

Before performing detailed spectral analysis, we have looked for any correlations between the soft (*ROSAT*) and hard (*RXTE*) X-ray count rates. The *ROSAT* and *RXTE* observations were not simultaneous, so to compare the two light curves we have linearly interpolated the *ROSAT* data to the time of the *RXTE* observations. The error for the shifted *HRI* points is the mean of the errors listed in Table 1. Fig. 2 shows the shifted *ROSAT* and unshifted *RXTE* count rates plotted against one another. A simple straight line model is not a good fit (reduced $\chi^2 \sim 2$). This may be a result of changes in the relative amounts of hard and soft components or spectral changes to a single component. Investigation shows that changes of ± 7 per cent in the hardness ratio cannot be ruled out. We have also, as a check, interpolated the *RXTE* data to the time of the *ROSAT* observations. The results are consistent with those (above and below) for the opposite case.

Of interest with respect to the soft excess is the intercept on the y-axis. If a single component spanned both the soft and hard X-ray bands, then the intercept would be expected to be at zero. However, if a soft excess were present then some residual soft count rate should remain, as the

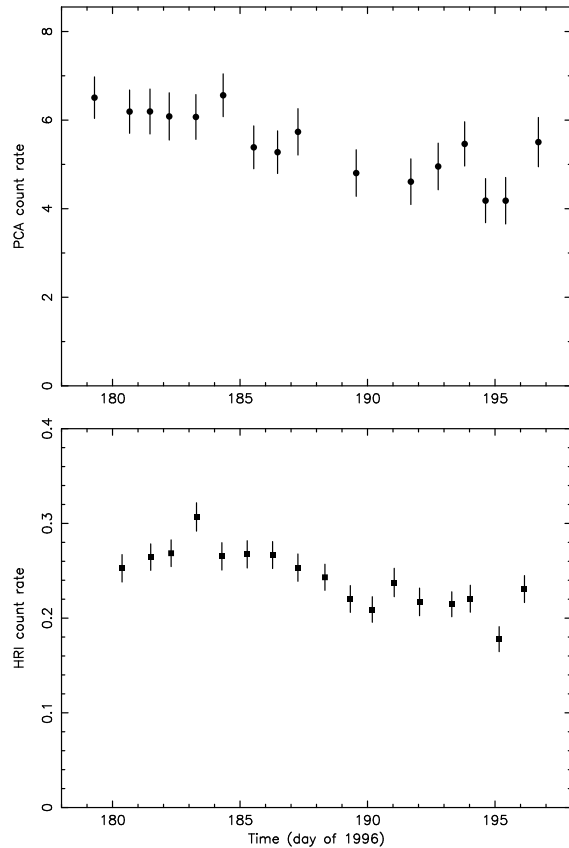


Figure 1. *RXTE* (top) and *ROSAT* light curves of 3C 279. The *RXTE* points include the effects of the background modelling discussed in Section 2

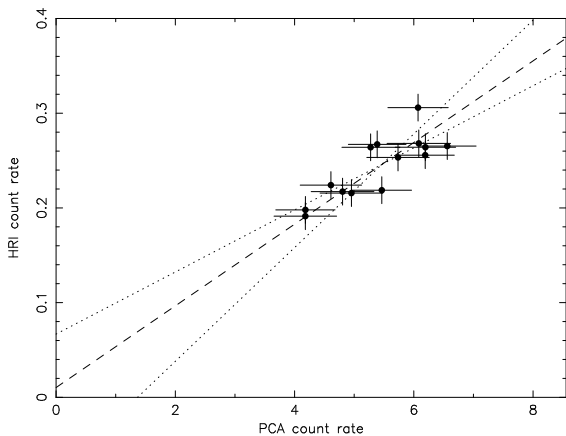


Figure 2. Shifted *HRI* vs unshifted *RXTE* count rate. The dashed line shows the best-fitting straight line model to the data. The dotted lines on the plots show the 68 per cent upper and lower bounds for this model.

hard band counts reduce to zero. The best-fitting models intersect the y-axis near zero, suggestive of no soft excess. However, the poorly sampled counts–counts plane and the large error bars give a mean 99 per cent upper limit on the residual *HRI* count rate of $0.15 \text{ counts s}^{-1}$. This is a sizable fraction of the observed *HRI* count rate, and only places a weak constraint on any soft excess of ≤ 60 per cent of the soft X-ray count rate.

4.2 Spectral fitting

Spectral analysis was performed using the XSPEC fitting package, with the results shown in Table 2. A power-law model with Galactic absorption (see Elvis, Lockman & Wilkes 1989) gives an acceptable fit to each *RXTE* observation. All the best-fitting indices are consistent with a single power law slope of $\alpha = 0.78 \pm 0.03$. This lies in the range measured by *ASCA* and *Ginga* (Tashiro et al. 1994; Lawson & Turner 1997).

The same model was applied to the combined *RXTE* and *ROSAT* data. We have treated the observations from each satellite as simultaneous if they were made within six hours of each other. If this was not the case, then the *RXTE* observation has been fitted separately with the two *ROSAT* observations (pre- and post-*RXTE*) closest to it, with the results being averaged (with errors added in quadrature). As with the *RXTE* data alone, a single power law is an acceptable fit in all cases. The errors on the derived spectral indices are much reduced due to the extended energy range, but again all the data are consistent with a single power law of $\alpha = 0.74 \pm 0.01$. This is consistent with that derived from the *RXTE* data alone, and means that the soft X-ray data are consistent with an extension of the hard X-ray power law into the *HRI* energy band.

However, as the *HRI* has no spectral capability a soft excess could still be hidden. To investigate this we produced a number of fake source spectra with two power law components: a hard component that is the average of the fits to the

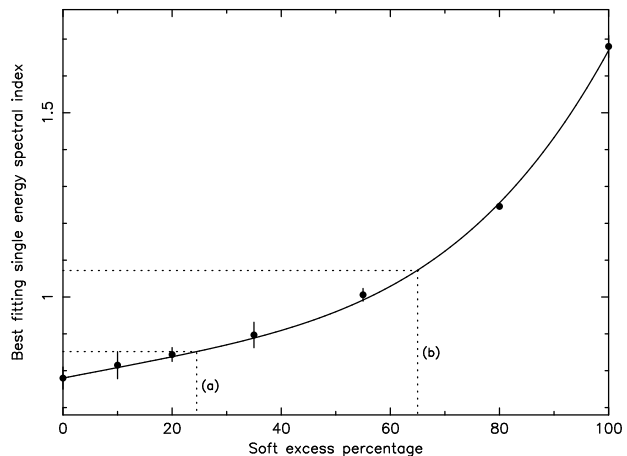


Figure 3. Plot of spectral index vs soft excess percentage derived from modelling. The data points represent the mean of the best-fitting indices for a particular strength of soft excess, the error bars are the standard deviation of these best fits (there are 20 model spectra per data point). Line (a) shows the upper limit for 3C 279 derived from the spectral fitting, while line (b) shows the expected spectral index if the soft excess were as prominent as that in 3C 273

RXTE data alone ($\alpha = 0.78$ with a flux at 1 keV of $3 \times 10^{-3} \text{ photons cm}^{-2} \text{ s}^{-1} \text{ keV}^{-1}$), and a soft component ($\alpha = 1.68$, the average value for the soft excess of 3C 273, Leach et al. 1995) with a varying normalisation. A single power law has then been fitted to these spectra (acceptably in each case) and the best-fitting spectral index measured. The results of the fitting are shown in Fig. 3. As expected, a larger fraction of soft excess results in a steeper single power law index.

The best-fitting spectral index to the combined *ROSAT* and *RXTE* data is $\alpha = 0.74 \pm 0.04$ (where the error is the standard deviation of the best fit values), and the 99 per cent, or 2.6σ upper limit is 0.84. This gives an upper limit to the luminosity of a soft excess of ~ 25 per cent of the total luminosity in the 0.1–2.0 keV band, or less than $3 \times 10^{38} \text{ W}$ ($q_0 = 0.5, H_0 = 50 \text{ km s}^{-1} \text{ Mpc}^{-1}$).

For comparison we have calculated (from Leach et al. 1995) that on average 73 per cent of the 0.1–2.0 keV luminosity of 3C 273 is from the soft excess. This is much larger than that seen in 3C 279. Red-shifting the spectrum of 3C 273 to the distance of 3C 279 only reduces the soft excess percentage to 65 per cent. If this percentage were actually present in 3C 279, we would expect an average spectral index of near $\alpha = 1.1$, a value some 8σ away from the observed value. This clearly shows that any soft excess in 3C 279 is intrinsically weaker relative to the hard X-ray power law than is seen in 3C 273.

5 CONCLUSIONS

We have presented contemporary *RXTE* (2–15 keV) and *ROSAT* (0.1–2 keV) observations of the quasar 3C 279 at daily intervals over a three week period. During this time the source exhibited only low amplitude variability, decreas-

Table 2. Spectral fitting results

N_X^a	α^b	χ_ν^{2c}	N_R^d	α^e	χ_ν^{2f}	S^g	S^h
1	0.82±0.08	0.5	1	0.69±0.03	0.6	12.8	8.3
2	0.68±0.11	1.1	1,2	0.70±0.05	1.0	12.3	8.1
3	0.58±0.13	0.6	2	0.72±0.04	0.6	12.1	8.2
4	0.80 ^{+0.17} _{-0.16}	0.8	3	0.75±0.04	0.8	11.8	8.5
5	0.68 ^{+0.13} _{-0.12}	0.9	4	0.80±0.04	0.9	12.1	9.5
6	0.83±0.10	0.8	5	0.70±0.03	0.8	13.0	8.6
7	0.99 ^{+0.13} _{-0.12}	0.5	6,7	0.80±0.05	0.6	10.8	8.5
8	1.02±0.12	0.6	7	0.81±0.04	0.7	10.7	8.6
9	0.66 ^{+0.15} _{-0.14}	0.7	8	0.72±0.04	0.7	11.5	7.9
10	0.45±0.18	0.2	10	0.75±0.05	0.3	9.5	6.8
11	0.68 ^{+0.20} _{-0.19}	0.9	12,13	0.80±0.07	0.9	9.0	7.1
12	0.65 ^{+0.19} _{-0.18}	0.4	13,14	0.73±0.07	0.4	9.8	6.8
13	0.96±0.14	0.7	15	0.70±0.04	0.8	10.9	7.2
14	0.73±0.19	0.7	15,16	0.77±0.07	0.6	8.3	6.2
15	0.82 ^{+0.22} _{-0.21}	0.6	16,17	0.77±0.08	0.6	8.5	6.4
16	0.76 ^{+0.20} _{-0.19}	0.5	17	0.71±0.05	0.5	10.8	7.3

Notes: ^a*RXTE* observation number, ^bbest-fitting power law slope to *RXTE* data only with 68 per cent error, ^cvalue for *RXTE* fitting only, ^d*ROSAT* observation numbers used in combined fits with the *RXTE* data, ^ebest-fitting power law slope to the combined *RXTE* and *ROSAT* data (see Section 4.2), ^fvalue for combined *ROSAT* and *RXTE* fits, ^g2–10 keV model flux, $\times 10^{-15} \text{ W m}^{-2}$, ^h0.1–2 keV model flux, $\times 10^{-15} \text{ W m}^{-2}$

ing in flux by ~ 30 per cent. The largely featureless nature of the light curves prevents us from determining any lag between the *RXTE* and *ROSAT* light curves which are quite consistent with zero time delay. We find no evidence for any spectral variability either within the *RXTE* observations or in the combined *RXTE* and *ROSAT* observations.

There is also no significant evidence that a soft excess is present, although modelling cannot rule out a soft excess which emits 25 per cent of the 0.1–2.0 keV X-ray luminosity. Comparison with 3C 273 shows that any soft excess is relatively weaker in 3C 279 than in 3C 273 (although the upper limit to the soft excess in 3C 279 in terms of absolute luminosity is some three times larger than that of 3C 273). This relative weakness could be caused by a number of phenomena, such as a more luminous source having a more massive black hole and cooler disc, but it is more likely that 3C 279 is more jet dominated than 3C 273, perhaps due to a higher beaming factor or more acute viewing angle.

REFERENCES

Arnaud K. A. et al., 1985, *MNRAS*, 217, 105
 Bradt H. V. D., Rothschild R. E., Swank J. H., 1993, *A&AS*, 97, 355
 Bühler P., Courvoisier T. J. L., Staubert R., Brunner H., Lamer G., 1995, *A&A*, 295, 309
 Comastri A., Setti G., Zamorani G., Elvis M., Giommi P., Wilkes B. J., McDowell J. C., 1992, *ApJ*, 384, 62
 Elvis M., Lockman F. J., Wilkes B. J., 1989, *AJ*, 97, 777
 Lawson A. J., Turner M. J. L., 1997, *MNRAS*, 288, 920
 Leach C. M., McHardy I. M., Papadakis I. E., 1995, *MNRAS*, 272, 221

Masnou J., Wilkes B. J., Elvis M., McDowell J. M., Arnaud K. A., 1992, *A&A*, 235, 5
 Mushotzky R. F., Done C., Pounds K. A., 1993, *ARA&A*, 31, 717
 Prieto M. A., 1996, *MNRAS*, 282, 421
 Saxton R. D., Turner M. J. L., Williams O. R., Stewart G. C., Ohashi T., Kii T., 1993, *MNRAS*, 262, 63
 Schartel N., Fink H., Brinkman W., Trümper J., 1992, in Brinkman W., Trümper J., eds, *X-ray and UV emission from Active Galactic Nuclei*. MPE, Munich, p. 195
 Schartel N., Walter R., Fink H. H., Trümper J., 1996, *A&A*, 307, 33
 Staubert R., 1992, in Brinkman W., Trümper J., eds, *X-ray and UV emission from Active Galactic Nuclei*. MPE, Munich, p. 42
 Tashiro M., Ueda Y., Kii T., Makino F., Fujimoto R., Mushotzky R., Makishima K., Yamashita A., 1994, in Makino F., Ohashi T., eds, *New Horizon of X-ray astronomy - First results from ASCA*. UAP, Tokyo, p. 343
 Turner T. J., Pounds K. A., 1989, *MNRAS*, 240, 833
 Turner M. J. L. et al., 1990, *MNRAS*, 244, 310
 Urry C. M., Arnaud K., Edelson R. A., Kruper J. S., Mushotzky R. F., 1989, in Hunt J., Battrick B., eds, *Proc. 23rd ESLAB symposium on Two Topics in X-ray Astronomy*. ESA SP-296, Noordwijk, Netherlands, p. 789